Journal of Controlled Release 226 (2016) 217–228

Contents lists available at ScienceDirect

Journal of Controlled Release

journal homepage: www.elsevier.com/locate/jconrel

Review article

Assessing biocompatibility of graphene oxide-based nanocarriers: A review

Siaw Fui Kiew [a], Lik Voon Kiew [b,*], Hong Boon Lee [a], Toyoko Imae [c,d], Lip Yong Chung [a,*]

[a] Department of Pharmacy, Faculty of Medicine, University of Malaya, 50603 Kuala Lumpur, Malaysia
[b] Department of Pharmacology, Faculty of Medicine, University of Malaya, 50603 Kuala Lumpur, Malaysia
[c] Graduate Institute of Applied Science and Technology, National Taiwan University of Science and Technology, 43 Section 4, Keelung Road, Taipei 10607, Taiwan, ROC
[d] Department of Chemical Engineering, National Taiwan University of Science and Technology, 43 Section 4, Keelung Road, Taipei 10607, Taiwan, ROC

ARTICLE INFO

Article history:
Received 5 January 2016
Received in revised form 6 February 2016
Accepted 6 February 2016
Available online 9 February 2016

Keywords:
Graphene oxide
Drug delivery
Tumor
Chemotherapy
Photodynamic therapy

ABSTRACT

Graphene oxide (GO)-based nanocarriers have been frequently studied due to their high drug loading capacity. However, the unsatisfactory biocompatibility of these GO-based nanocarriers hampers their use in clinical settings. This review discusses how each of the physicochemical characteristics (*e.g.*, size, surface area, surface properties, number of layers and particulate states) and surface coatings on GO affect its *in vitro* and *in vivo* nanotoxicity. We provide an overview on the effect of GO properties on interactions with cells such as red blood cells, macrophages and cell lines, and experimental organisms including rodents, rabbits and Zebrafish, offering some guidelines for development of safe GO-based nanocarriers. We conclude the paper by outlining the challenges involving GO-based formulations and future perspectives of this research in the biomedical field.

Contents

* Corresponding authors.
E-mail addresses: lvkiew@um.edu.my (L.V. Kiew), chungly@hotmail.com (L.Y. Chung).

http://dx.doi.org/10.1016/j.jconrel.2016.02.015
0168-3659/

1. Introduction

The carbon-based nanomaterials have been one of the focal points on the scientific stage since the discovery of fullerene in 1985, carbon nanotubes (CNTs) in 1991 and then followed by graphene in 2004 [1,2]. Before 2004, graphene was only a scientific model and was literally the mother element of other well-known carbon-based nanomaterials — graphite, diamond, nanoribbons, CNTs and fullerenes (Fig. 1). It was not until 2004, graphene was proved to be thermodynamically stable under ambient conditions, thanks to Andre Geim and Konstantin Novoselov — winners of the Nobel Prize in Physics 2010 [1]. In recent years, the research efforts invested in excavating the potential applications of graphene in the field of biomedicine [3–12] have gradually exceeded the fullerenes [2] and are expected to match those of the CNTs in the near future [13,14].

Graphene is a one-atom-thick, two-dimensional (2D) planar sheet (0.35–1.6 nm in thickness) that possesses trigonally bonded sp^2 carbon atoms that are tightly organized into a honeycomb crystal lattice [15]. The large surface area of graphene which is doubled compared to CNTs, has made it a good drug carrier candidate. However, the use of graphene as a drug carrier has been hampered by its high aggregation tendency due to its hydrophobic nature. It was not until 2008 that Dai's group [16] overcame the aggregation issue of graphene by using the oxidized form of graphene — graphene oxide (GO) (Fig. 2). In comparison to other carbon-based nanomaterials such as CNTs, GO exhibits some merits like low cost of production [16,17], extremely large surface area for efficient drug binding and lesser toxic metallic impurities from fabrication process [13]. In fact, GO derivatives are reported to have notably improved tumor passive targeting effect and higher tumor uptake *via* the enhanced permeability and retention (EPR) effect compared to CNTs, probably attributed to the unique 2D structure and small lateral size [18].

The unique properties of GO such as high drug loading capacity [19] have sparked growing interests in biomedical field but its safety considerations are still posing a myriad of unanswered questions. Until now, biological investigations of GO, both *in vitro* and *in vivo* have no consensus results and sometimes the results are in contradiction. The method of production, chemical characterization and biomedical applications of GO have been extensively reviewed [2,18,20–28]. There is still a lack of systematic review on the structure–activity relationship between the

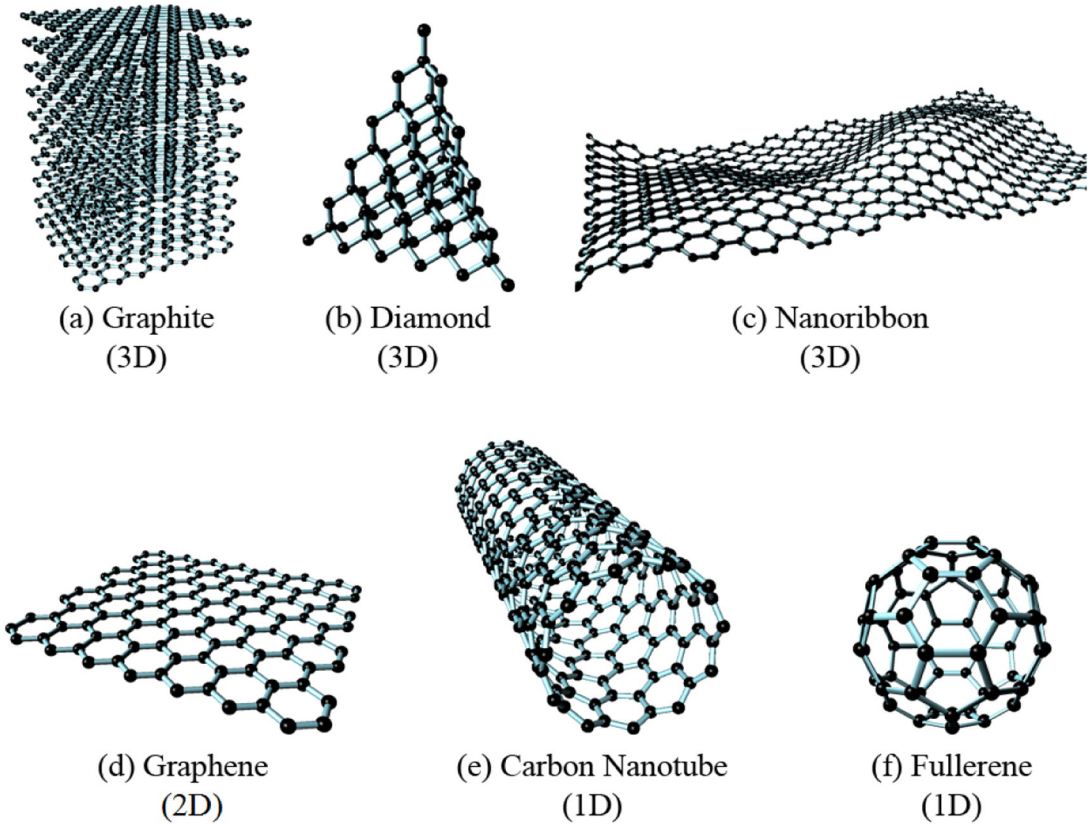

Fig. 1. Carbon-based nanomaterials.

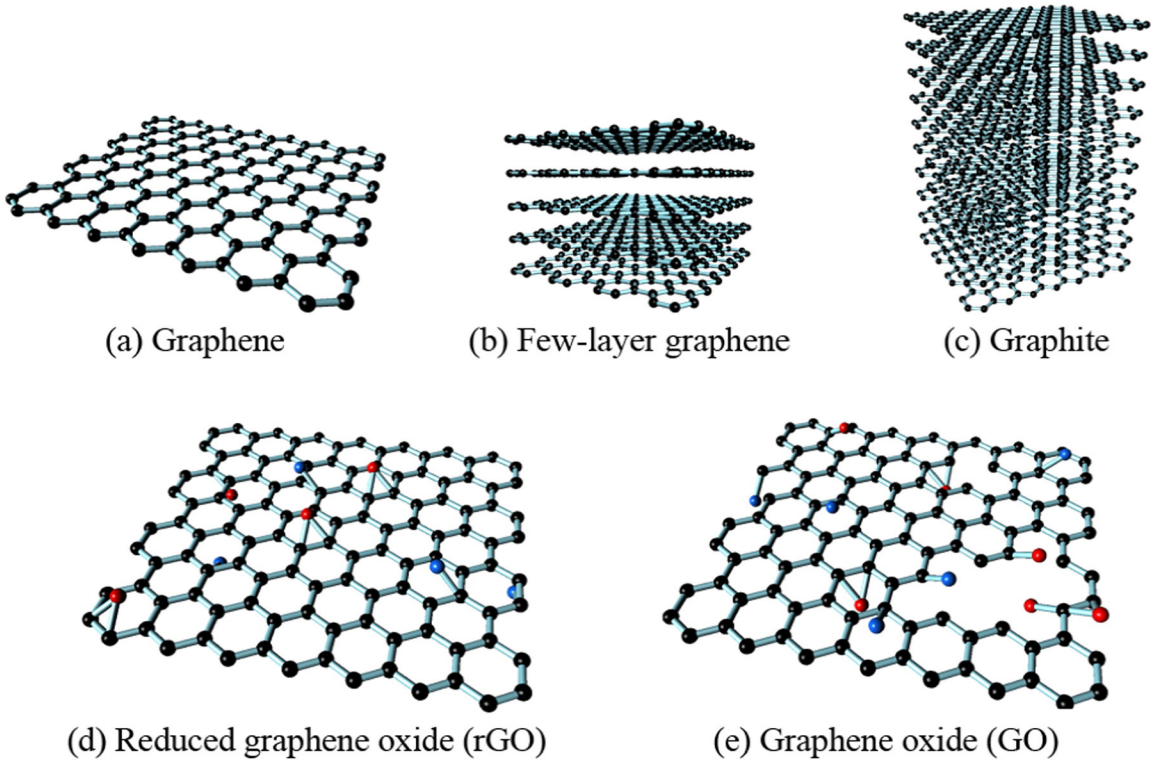

Fig. 2. Graphene family nanomaterials.

properties of GO and interactions with organism. This paper attempts to offer some guidelines at this infancy stage to assist the development of safe GO-based nanocarriers.

In this paper, we start the discussion with the properties of GO that qualify it as a potential drug carrier. Then, we discuss in detail how each of the physicochemical characteristics of GO – size, surface charge, particulate state, number of layers – as well as surface coatings affect the *in vitro* and *in vivo* behaviors of GO-based formulations. At the end of the paper, we delineate the challenges and safety issues associated with GO and the future perspectives of GO research.

1.1. Graphene oxide (GO)

Graphene oxide (GO) (Fig. 2(e)) has a structure similar to that of pristine graphene (Fig. 2(a)) but features a variety of chemically reactive functionalities — epoxy (–O–), hydroxyl (–OH) and carboxylic acid (–COOH) groups [29,30]. This highly oxygenated amphiphilic sheet contains a large hydrophobic basal plane and hydrophilic edges. In contrast to graphite oxide, which has more than 10 layers arranged in a crystalline structure, GO exists in monolayers or a few layers (maximum up to 10 layers) [31] with defects randomly spread on the large basal structure. The thickness of a single-layer GO is usually between 1 to 1.4 nm [32]. This thin layer provides flexibility to the GO that allows it to be folded into a gauzelike shape in a biological medium [31] or during the cellular internalization process [33].

1.2. Properties of GO as a drug carrier

GO has several prominent properties relevant to biological applications particularly for use as an anticancer drug nanocarrier [34].

1.2.1. Large surface area

Unlike other carbon-based nanomaterials, two-dimensional (2D) GO has both single sheet surfaces and edges that are accessible for biomolecular interactions. The surface area of GO is approximately 2600 m^2/g, at least an order of magnitude higher than the surface area of most other nanomaterials [17,35,36]. This enormous surface area endows GO with a high drug loading capacity [17,37,38]. For example, a drug loading of 235 wt.% has been reported on GO [19]. This value is far greater than the loading value of other nanomaterials such as polymer micelles [39] and liposomes [40] which have a loading capacity that is usually below 10%.

1.2.2. Unique surface properties

In contrast to the hydrophobic nature of pristine graphene that easily causes irreversible agglomeration [15] and a large amount of protein adsorption [23], GO contains both hydrophobic graphenic domains and hydrophilic edges that provide an amphiphilic characteristic to this material. The former is important for carrying water-insoluble dye molecules and drugs through non-covalent bonding — π–π stacking or hydrophobic interaction or hydrogen bonding [23]. The latter serves as anchor sites for functionalization [15,41] and provides pH-dependent negative surface charges to maintain colloidal stability [42].

1.2.3. Good water dispersibility

Water dispersibility of a drug carrier is fundamental and important for applications in life sciences [43]. GO has good water dispersibility and is generally considered better than CNTs [13]. GO dispersed in water has a negative surface charge due to ionization of the carboxylic acid and hydroxyl groups; the negative surface charge is high enough to create electrostatic repulsion that provides stable dispersion of GO in water [42].

1.2.4. pH-sensitive zeta potential

The zeta potentials of GO suspensions are pH sensitive. GO sheets can form a stable suspension at pH values ranging from 3 to 12 with the best stability at pH 7 or 8 [44]. Through proper tuning of this unique property, GO can be formulated into a smart system that has controlled release property in various specific microenvironments (*e.g.*, weak acidity) that differentiate cancer tissue from normal tissue. For example, GO has been reported to give a higher drug release at acidic pH compared to neutral pH [19].

1.2.5. Unique intrinsic optical properties

GO possesses unique intrinsic optical properties including near-infrared photoluminescence (570 nm) (for live cell imaging) [33,45,46] and optical absorptions (for photothermal therapy) [47–49]. The photoluminescence of GO could allow direct tracking of the intracellular location of GO-based nanoparticles without requiring the conjugation of foreign fluorescence moieties. Interference during imaging is also minimized because of minimal cellular autofluorescence in the NIR region [45].

1.3. Limitations of GO

GO has great potential as a drug carrier if the limitations in its properties could be addressed and the knowledge gap in GO-related biomedical research could be filled.

1.3.1. Aggregation in biological solution

GO disperses well in water but aggregates in salted environments, such as phosphate buffered saline (PBS) [16] and protein rich cell culture medium. Salts, such as NaCl, $MgCl_2$ and $CaCl_2$ greatly destabilize GO [50]. GO aggregates and settles out in PBS and culture medium because the ionic strength of the salts [51] and the non-specific binding of the protein [18] shield the electric double layer of GO.

1.3.2. Non-uniform size

GO sheets rarely appear in one uniform size [17]. The wide distribution of sizes of GO might affect the biocompatibility of GO sheets as well as leading to non-consensus results, both *in vitro* and *in vivo*. Sometimes, it is the chemical impurities retained in GO [33] or the different types of testing models used in *in vitro* and *in vivo* settings that lead to inconsistencies in the biological assessment.

1.3.3. Knowledge gap in GO-related biomedical research

The controlled release capability of GO triggered by different stimuli such as NIR light, pH and electricity has been studied [52–56] but the studies have yet been carried out *in vivo*. The *in vivo* behaviors of GO such as blood circulation time, inflammation response and clearance of GO nanocarriers are not clearly understood due to limited researches in these areas [37,57]. Also, study on the underlying mechanism of GO-induced pulmonary toxicity [58,59] has not been determined definitively.

2. *In vitro* and *in vivo* biocompatibility of GO-based formulations

As a drug carrier, GO would be in contact with human organs and cells. Titov and co-workers [60] demonstrated by using dynamic simulation that graphene family nanomaterials interact with lipids without any significant perturbation of the phospholipid bilayer. However, how the intrinsic properties of GO affect cellular responses and the behavior of GO in a real biological environment are still poorly understood. Therefore, effort in filling the knowledge gap as to the extent of the toxicological risks caused by GO nanomaterials is urgently needed.

2.1. In vitro biocompatibility

Table 1 lists different GO-based formulations according to size and the *in vitro* model utilized in the biocompatibility testing. The *in vitro* biocompatibility tests generally involve red blood cells, phagocytes (macrophage) and non-phagocytic cells (endothelial and tumor cells) [33], which come into contact with the administered GO. Off note, different from the classification framework for graphene-based materials by Wick et al. [61], micro-sized and nano-sized GO sheets here refer to GO with lateral dimension in micrometer range and nanometer range, respectively.

2.1.1. Hemocompatibility

Hemocompatibility investigation is an important toxicity assessment for biomedical applications that involves intravenous injections because red blood cells (RBCs) are one of the primary sites of interaction upon administration. The hemocompatibility studies of plain nano-sized GO started in the year 2011 [51,59].

Nano-sized GO (350 nm) was found to induce a severe hemolysis effect (70% hemolysis at 25 μg/mL) compared to micro-sized (3 μm) graphene sheets (10% hemolysis at 100 μg/mL) after 3 h of incubation [51]. The serious RBC membrane disruption by GO was attributed to the strong electrostatic interactions between the negatively charged GO surface and the lipid bilayer of RBC membrane [51,65]. In contrast, the good hemocompatibility of micro-sized graphene sheets was most likely due to the lower overall surface area of aggregated graphene sheets available for interaction with RBCs. The author claimed that individually dispersed GO samples were more toxic than the aggregated carbon nanomaterials, and similar results were previously reported for CNT nanocarriers [51,75]. Despite the lower hemolysis effects of micro-sized graphene sheets, hemagglutination was observed around the graphene sheet aggregates [51]. Interestingly, when a GO sample consisted of a wide size distribution (10–800 nm), the hemolysis effect was greatly suppressed to below 10%, even for concentrations up to 80 μg/mL [59]. The inconsistency of the results remains unclear and requires further investigation.

A proper surface coating can remarkably improve GO hemocompatibility. For example, coating GO with chitosan (CS) (by electrostatic adsorption) [51], bovine serum albumin (BSA) and heparin (Hep) [65] nearly eliminated the hemolytic activity. Biopolymer coatings might serve as a protecting layer or create electrostatic repulsions that reduce the contact between GO and RBCs, thus mitigating the toxicity of GO to RBCs [51,65].

Another possible reason for the higher hemocompatibility of GO/CS is the pH-responsive conformational change of CS. GO/CS dispersed well in acidic water (pH ~4.8) but rapidly aggregated in PBS (pH ~7.4) [51]. The GO/CS aggregates had a smaller interaction surface with RBCs and thus, a decreased hemolysis effect.

The aggregation of blood cells caused by GO was reduced by adding 1% Tween 80 surfactant, which could greatly attenuate the interaction between GO and blood cells [64].

2.1.2. Inflammation responses

Macrophages play an important role in non-specific immune defense by engulfing foreign substances through phagocytosis, but they also establish a substantial barrier against intravenously injected GO nanocarriers. GO nanocarriers have high possibility of being cleared out by macrophages before reaching the targeted site or induce an inflammation response.

Yue et al. [33] compared the cellular responses of 2 μm GO and 350 nm GO in two types of cells — phagocytes and non-phagocytes. They found that macrophages had higher uptake capability than that of non-phagocytes, most likely because the former could overcome the strong electrostatic repulsions between GO (negatively charged carboxyl group) and the negatively charged cell surface *via* the Fcγ receptor-mediated phagocytosis pathway [33].

Both micro-sized and nano-sized GO sheets led to similar cellular uptake by macrophages but the micro-sized GO activated stronger inflammation responses as evidenced by remarkable increases in the levels of many cytokines (IL-6, IL-12, TNF-α, MCP-1 and IFN-γ) [33]. The author postulated that the powerful immune response from macrophages was most likely due to the strong steric effects imposed by the micro-sized GO upon cellular internalization [33]. Ma et al. reported a similar finding as they claimed that larger GO enhanced the production of inflammatory cytokines and recruitment of immune cells due to a stronger interaction with toll-like receptors on plasma membrane and activation of NF-kB pathway [76].

Table 1
In vitro biocompatibility studies of GO-based nanocarriers.

GO-based formulation	Targeting molecule	Size of GO	Cell type	Ref.
GO	–	2 μm & 350 nm	PMØ (peritoneal macrophage) J774A.1 (murine macrophage) LLC (murine Lewis lung carcinoma) MCF-7 (human breast cancer) HepG2 (human hepatocarcinoma) HUVECs (human umbilical vein endothelial cells)	[33]
	–	~1–5 μm	HDF(human fibroblast) MGC803 (human gastric cancer) MCF-7 (human breast cancer) MDA-MB-435 (human breast cancer) HepG2 (human hepatocarcinoma)	[58]
	–	~1 μm	ARPE-19 (human retinal pigment epithelial)	[62]
	–	780 ± 410 nm 430 ± 300 nm 160 ± 90 nm	A549 (human lung adenocarcinoma)	[63]
	–	~350–780 nm	RBC (human red blood cell) CRL-2522 (human skin fibroblast)	[51]
	–	10–800 nm	Sprague–Dawley rats erythrocyte	[59]
	–	205.8 nm 146.8 nm 33.8 nm	HeLa cell (human cervical adenocarcinoma)	[34]
GO and GO/Ag	–	~1 μm	HT-29 (colorectal adenocarcinoma)	[43]
GO/Tween 80	–	300–1000 μm	Balb/c mice blood cells	[64]
GO/BSA and GO/Hep	–	~1 μm	HUVECs (human umbilical vein endothelial cells) RBC (human red blood cell)	[65]
GO/BSA	–	~400–1200 nm	C2C12 (mouse mesenchymal progenitor)	[31]
GO–FBS	–	~1 μm	A549 (human lung adenocarcinoma)	[66]
GO–1PEG	–	<40 nm	A549 (human lung adenocarcinoma)	[17]
GO–1PEG and GO–6PEG	–	95 nm 190 nm	Saos-2 (human osteoblast) MC3T3-E1 (murine preosteoblasts) L929 (murine fibroblast) RAW-264.7 (murine macrophages)	[48]
GO–1PEG and GO/1PEG	RGD	20 nm 18.8 nm	U87MG (human glioblastoma cells)	[67]
GO–6PEG	TRC105	~10–50 nm	HUVECs (human umbilical vein endothelial cells) MCF-7 (human breast cancer)	[68]
GO–DEX	–	~50–100 nm	HeLa cell (human cervical adenocarcinoma)	[69]
	–	~2 μm	HeLa cell (human cervical adenocarcinoma)	[70]
	Fe	174.4 nm	HeLa cell (human cervical adenocarcinoma)	[71]
GO–G4–Cy	Fe	~50 nm	MCF-7 (human breast cancer) MDA-MB-231 (human breast cancer)	[47]
GO–GOH	FA	~6.4 μm	HeLa cell (human cervical adenocarcinoma)	[72]
GO/F127	–	~350 nm	HeLa (human cervical adenocarcinoma)	[73]
GO–TiO_2	–	~1 μm	HeLa (human cervical adenocarcinoma)	[74]

Symbols: GO = graphene oxide, Ag = silver, BSA = bovine serum albumin, Hep = heparin, FBS = fetal bovine serum, 1PEG = linear poly(ethylene glycol), 6PEG = branched poly(ethylene glycol), RGD = arginine–glycine–aspartate peptide, TRC105 = CD105 endoglin targeting human/murine chimeric IgG1 monoclonal antibody, DEX = dextran, Fe = Fe_3O_4, G4 = 4th generation amine-terminated poly(amido amine) dendrimer, Cy = cyanine 5.0, GOH = hydroxyl-terminated poly(amido amine) dendrimer, F127 = pluronic, TiO_2 = titanium oxide. Chemical bonds: – indicates covalent bonding and / indicates noncovalent bonding in the GO-based formulation.

The similarity of the cellular uptake by macrophages for both micro-sized and nano-sized GO sheets might be due to similar total surface area of the GO sheets per equal quantity amount [33]. Accordingly, both GO sheets absorbed equal amounts of IgG opsonin and were thus internalized by macrophages at a similar level through IgG–FcγR-mediated phagocytosis [33]. Additionally, some micro-sized GO sheets were reported to be transported into acidic lysosomes [33], possibly to be digested by lysosomes.

Phagocytosis is an energy-dependent process. At 37 °C, the internalization of GO (both micro- and nano-sized) into phagocytes was at least two-fold faster than the GO internalization at 4 °C (approximately 20% cellular internalization) [33].

These findings indicated that nano-sized GO was a more suitable carrier in terms of avoiding inflammation response. In fact, according to Vila et al. [48] and Stolnik et al. [77], the macrophage recognition of nanomaterials could be reduced by maintaining the particle size at approximately 150 nm and by conferring the nanomaterial with hydrophilic surfaces that would weaken the opsonin–protein interaction.

2.1.3. Cytotoxicity

The testing of the GO cytotoxicity in mammalian cells showed that micro-sized GO led to higher cytotoxicity than nano-sized GO likely due to the faster sedimentation rate and the formation of compact GO aggregates on top of the adherent cells in the wells, inhibiting the nutrient availability for the growth of cells [51]. Generally, GO exhibited dose-dependent toxicity [51,58,59,62,63]. At concentrations greater than 50 μg/mL, micro-sized GO showed obvious toxicity to both normal and tumor human cells, including breast cancer, hepatocarcinoma, umbilical vein endothelial cells, gastric cancer and fibroblast cells [33,58]. For example, GO (1–5 μm) significantly reduced the cell viability of human skin fibroblasts (CRL-2522), human dermal fibroblasts (HDFs) and human retinal pigment epithelial (ARPE-19) cells to ~30–75% viability after 24 h of incubation [51,58,62]. Similar phenomena were also observed in other cell lines such as MGC803, MCF-7, MDA-MB-435 and HepG2 cells [58].

In contrast, Liao et al. [51], Chang et al. [63] and Li et al. [78] reported that nano-sized GO with sizes ranging from 430 nm to 780 nm was less toxic to fibroblast cells, A549 cells and GLC-82 cells, with a survival rate

exceeding 80% at the high concentration of 200 μg/mL. Recently, Zhang et al. [34] reported that nano-sized GO in the range of 33 nm to 205 nm at a concentration of 100 μg/mL inhibited approximately 50% to 90% of the HeLa cell viability after 24 h of treatment. The smaller GO (33 nm) produced 40% less cytotoxicity compared with that of 205 nm GO. According to the author, this result most likely occurred because the larger sized GO nanosheets caused more severe physical damage to the cell membrane [34].

The cellular uptake of nano-sized GO by HeLa cells was also size-dependent, with smaller GO nanosheets having higher cellular uptake [34]. In fact, the optimum size of particles for faster cellular uptake was reported to range from 100–200 nm [79].

In conclusion, nano-sized GO is preferred over micro-sized GO as a carrier with a lower toxic level, weaker inflammation response and better cellular uptake. However, there are inconsistencies in evaluations of the size dependence cytotoxicity [34,63]. This might be due to variations in GO preparation and the types of cells used in *in vitro* testing [63]. Fig. 3 below provides a schematic overview of how the intrinsic properties of GO affect its *in vitro* biocompatibility.

2.2. In vivo biocompatibility

Table 2 below lists different GO-based formulations whose *in vivo* biocompatibilities have been investigated; these properties include toxicity, pathological changes, inflammation response and clearance from the body.

2.2.1. In vivo toxicity

The toxicity of plain GO was investigated in Zebrafish [88], Kunming mice [58,59], C57/B6 mice [33] and Japanese white rabbits [62].

Microinjection of nano-sized GO (99 nm) into Zebrafish induced apoptosis and thus morphological defects in a dose-dependent manner, whereas GO–PEG (301.3 ± 87.2 nm) significantly attenuated its toxicity [88]. However, both GO and GO–PEG caused similar degree of angiogenic defect and the underlying mechanism was not clear. In mice, the drug-loaded GO-PEG could effectively destroy the tumor with no tumor recurrence observed in the next 40 days [86], and the treated mice had a nearly two-fold longer life span than mice treated with free drug [85]. Importantly, when severe lesions were found in the heart tissue of mice treated with free DOX, histology analysis showed that GO–PEG/DOX caused only little cell denaturation of heart tissue [86].

2.2.2. Pathological changes

Generally, both micro- and nano-sized GO sheets primarily accumulated in the lungs, liver and spleen at dosages of 0.2 to 0.5 mg per mouse [58,59,89], with a much longer retention time of up to one month in the lungs [58]. This accumulation induced significant pathological changes in the lungs, including strong dose-dependent inflammatory cell infiltration, pulmonary edema and granuloma formation [58,59]. Intravenous administration of micro-sized GO resulted in lung occlusion within 1 min, likely due to the particulate aggregation [89]. The uptake of GO in the liver and spleen indicated that the uptake of GO was also intercepted by the mononuclear phagocytes in the reticuloendothelial system (RES) [59]. Fortunately, nano-sized GO did not exert a significant pathological influence on the liver, spleen and kidney, suggesting that nano-sized GO was biocompatible with most organs, although lung pathologies still occur at high doses (0.4 mg per mouse) [59].

A dextran (DEX) coating caused GO–DEX to dominantly accumulate in the liver and spleen with no obvious toxicity noticed in the organs [69], in contrast to the dominant uptake of plain GO in the lungs which led to obvious pulmonary toxicity [58]. The potential risk of GO to the lung also could be reduced by adding 1% Tween 80 to the GO suspension [64]. GO/Tween 80 tended to accumulate in the liver due to its greater mobility in the circulatory system. According to the author, the GO/Tween 80 formulation greatly altered the biological performance of GO and caused no histological alterations of blood cells, spleen, brain and testes [64].

2.2.3. Inflammation response

Yue et al. [33] demonstrated that micro-sized plain GO (2 μm) caused a more severe inflammation response compared with nano-sized GO (350 nm) upon subcutaneous injection into the neck region

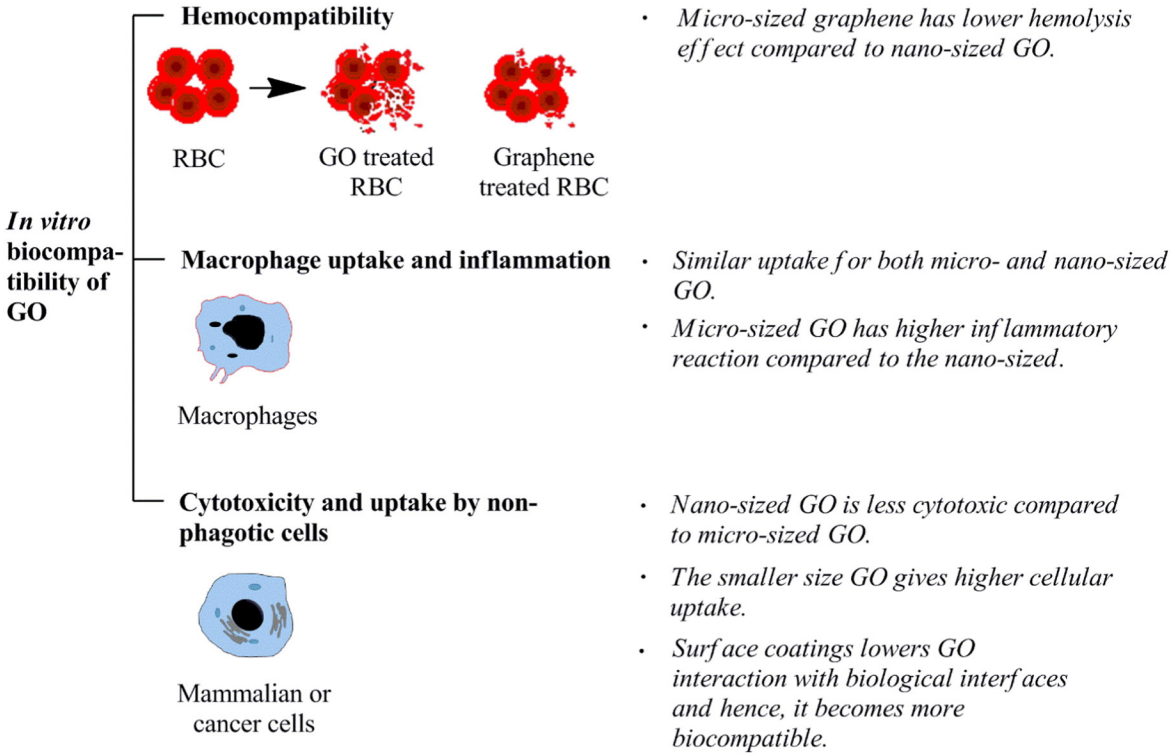

Fig. 3. *In vitro* biocompatibility of GO: hemocompatibility, macrophage uptake, immune response, cytotoxicity and cellular uptake.

Table 2
Preclinical studies of GO-based nanocarriers.

GO-based formulation	Drug*/photosensitizer**	Targeting molecule	Size of GO	Animal model	Ref.
GO	–	–	~1–5 μm	Kunming mice	[58]
	–	–	2 μm & 350 nm	C57/B6 mice	[33]
	–	–	10–800 nm	Kunming mice	[59]
	–	–	~1 μm	Japanese white rabbit	[62]
	–	Trastuzumab	64 nm	Balb/neuT mice Balb/c nu/nu mice	[80]
	Doxorubicin*	HA	10–200 nm	H22 hepatic cancer cell-bearing Kunming mice	[81]
GO–6PEG	–	–	~25–50 nm	Balb/c mice	[82]
	–	TRC105	~10–50 nm	4 T1 murine breast tumor-bearing mice	[68]
	Doxorubicin*	Transferrin	100–400 nm	Sprague–Dawley rats	[83]
	Doxorubicin*	IONP	~50–300 nm	4T1 murine breast tumor-bearing Balb/c mice	[84]
GO–1PEG	HPPH**	–	<50 nm	Athymic nude mice	[85]
	Doxorubicin*	–	~100 nm	EMT6 tumor-bearing mice	[86]
GO–DEX	–	–	~50–100 nm	Balb/c mice	[69]
GO/Ag	Doxorubicin*	NGR	–	S180 tumor-bearing Balb/c mice	[87]
GO/Tween 80	–	–	300–1000 nm	Balb/c mice	[64]

Symbols: GO = graphene oxide, HA = hyaluronic acid, 6PEG = branched poly(ethylene glycol), TRC105 = CD105 endoglin targeting human/murine chimeric IgG1 monoclonal antibody, IONP = iron oxide nanoparticle, 1PEG = linear poly(ethylene glycol), HPPH = (2-(1-hexyloxyethyl)-2-devinyl pyropheophorbide-alpha), DEX = dextran, Ag = silver, NRG = Asn-Gly-Arg peptide. Chemical bonds: — indicates covalent bonding and / indicates noncovalent bonding in the GO-based formulation.
Asterisk: * indicates chemotherapeutic drug and ** indicates photosensitizer.

of mice. A large number of mononuclear cells and tissue impairment were observed in the harvested neck adipose tissues injected with 2 μm GO. A recent study reports a similar result in which the micro-sized GO induced a classic foreign body response [89]. In another study, Yan et al. [62] studied the intraocular biocompatibility of micro-sized (~1 μm) GO. The rabbit eyes injected with 0.3 mg of GO were clear with no inflammation responses for 49 days but the GO might have diffused to the vitreous region of the eye [62]. PEGylated GO showed no noticeable sign of inflammation in major organs of the treated mice [82].

2.2.4. Clearance

Size, rather than surface coatings, determines the clearance pathways of GO-based formulations. Nano-sized GO (usually smaller than 10 nm) was quickly eliminated through renal routes [59], whereas micro-sized GO was preferentially expelled by liver secretion into the biliary tract system [58]. For example, GO–PEG conjugates whose sizes were larger than the cut-off of renal filtration (~5 nm) were cleared through the hepatobiliary pathway [68]. However, GO–DEX with a wide size distribution (~50–100 nm) had two different clearance pathways. Ultra-small GO–DEX was excreted in urine *via* the renal pathway,

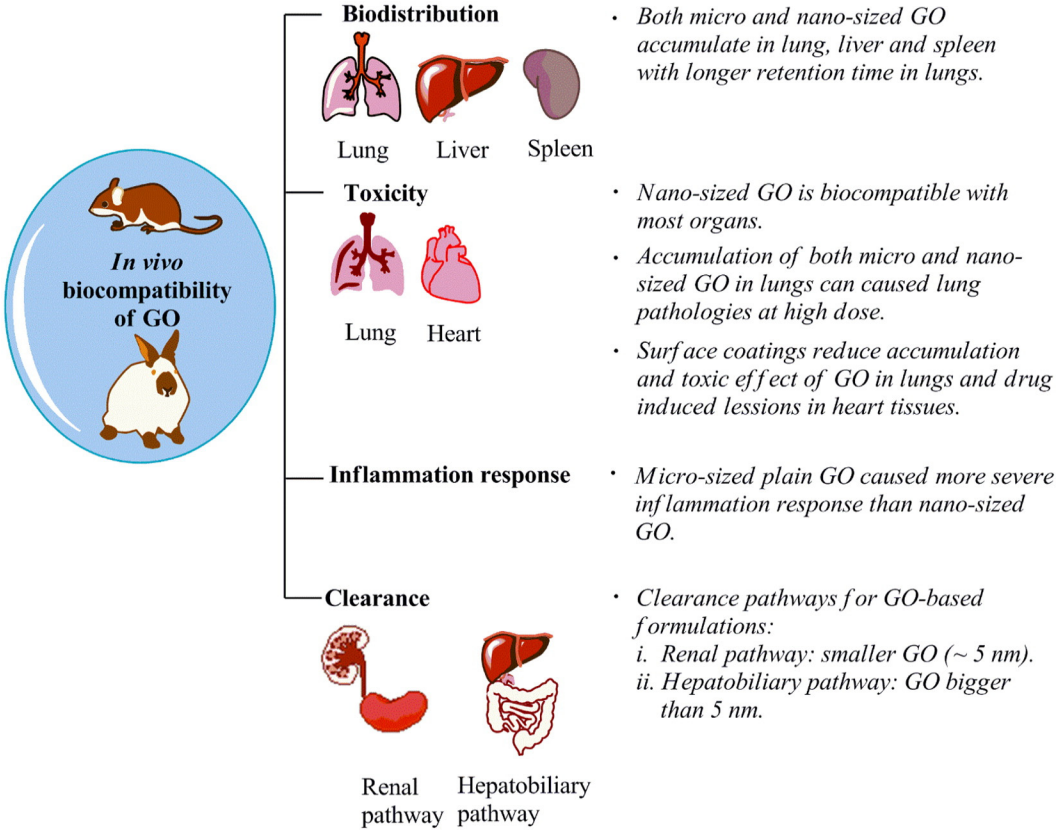

Fig. 4. *In vivo* biocompatibility of GO: biodistribution, toxicity, inflammation response and clearance.

whereas larger GO–DEX was excreted *via* the fecal pathway [69]. Interestingly, the majority of GO–DEX was cleared from Balb/c mice within one week and did not cause any obvious abnormality in various organs of the treated mice [69]. Fig. 4 below gives an overview of the *in vivo* (preclinical) studies of GO, offering some guidelines to develop safe GO-based nanocarriers.

In conclusion, coatings with biopolymers and surfactant could strikingly change the biocompatibility and biodistribution of GO. Therefore, surface functionalization is important to make GO highly biocompatible while also retaining its excellent properties for a drug delivery system. Nevertheless, biocompatibility assessment of GO is still limited. Further intensive investigation of the GO *in vivo* behavior, biodistribution and long-term toxicity is in high demand. Table 3 provides an overview of *in vitro* and *in vivo* cellular responses of the GO-based formulations based on factors such as size, surface coating, number of layer, particulate state and surfactant.

3. How different surface coatings address biocompatibility issue of GO

For attempts to fully utilize the excellent properties of GO as a drug nanocarrier without being hampered by their inherent weakness such as cytotoxicity at high concentration and preferential lung accumulation, several strategies have been proposed. The most convenient and efficient method involves surface functionalization of GO *via* either covalent or noncovalent conjugation [22,31,64,67,90]. In the following section, we discuss several surface coatings that have been studied to improve the biocompatibility of GO nanocarriers. Among the surface coatings, poly(ethylene glycol) (PEG) is the most often used polymer but its cost of production is relatively high [91]. This has encouraged researchers to explore other biocompatible surface coatings.

3.1. Bovine serum albumin (BSA)

Bovine serum albumin (BSA) in cell culture medium can affect the cellular uptake, intracellular localization and biocompatibility of nanomaterials [92]. If serum is used, opsonin proteins, such as immunoglobulins, that are coated on nanomaterials can activate phagocytosis [92]. BSA proteins that are adsorbed on nanomaterials could also mitigate cell cytotoxicity by lessening the contact between nanomaterials and cells [34,92]. In another instance, heat inactivation of the serum, which is typically performed during medium preparation might cause complement depletion, leading to conflicting outcomes for the same materials [92]. Therefore, the cell culture conditions should be carefully controlled when assessing the biocompatibility of nanomaterials so that the obtained results can be reasonably extrapolated to both *in vitro* and *in vivo* scenarios.

Table 3
In vitro and *in vivo* cellular response of GO-based formulations.

Factors	*In vitro* biocompatibility	Ref.	*In vivo* biocompatibility	Ref.
Size	Hemocompatibility: • Micro-sized graphene has lower hemolysis effect compared to nano-sized GO, due to electrostatic interaction. • Micro-sized graphene induced hemagglutination.	[51,59,65]	Inflammation responses: • Micro-sized GO causes more severe inflammation response than nano-sized GO. • Micro-sized GO causes no inflammation response in rabbit eyes.	[33,62]
	Inflammation responses: • Micro-sized GO induces stronger inflammation response, due to steric effect or stronger interaction with toll-like receptors on plasma membrane, thus activating NF-kB pathway. • Micro-sized GO is possible to be digested by lysosome, due to lysosome co-localization.	[33,48,76,77]	Pathology changes: • Both micro- and nano-sized GO cause pulmonary edema and granuloma formation in the lung, due to retention time of up to 1 month. • Micro-sized GO causes lung occlusion within 1 min. • Nano-sized GO has no toxic effect on the liver, spleen and kidney.	[58,59,89]
	Cytotoxicity: • Micro-sized GO has higher toxicity, due to faster sedimentation rate and thus inhibiting the nutrient available for cells or due to micro-sized GO causing more severe physical damage.	[33,51,58,62]	Clearance: • Micro-sized GO accumulates in the liver and biliary tract system while nano-sized GO accumulates in the urine. • Nano-sized GO (<5 nm) is eliminated through renal route while bigger sized GO (~50–100 nm) is eliminated through both renal and fecal pathways	[58,59,69]
Surface coating	Hemocompatibility • Surface coatings mitigate hemolysis effect by acting as protecting layers or exerting repulsion force or forming aggregate to reduce GO–cell contact.	[51,65]	Toxicity: • Surface coated GO accumulates in the liver and spleen, and gives no obvious toxicity. • Surface coating attenuates GO-induced apoptosis in Zebrafish. • Surface coated GO causes only little cell denaturation of heart tissues compared to drug alone. Inflammation responses: • Surface coated GO shows no noticeable sign of inflammation in major organs.	[69,86,88] [82]
Number of layer	Inflammation responses: • Both micro- and nano-sized GO with similar amount of layers have similar macrophage uptake level.	[33]		
Particulate state	Hemocompatibility: • Aggregation in micro-sized GO and in some surface coated GO reduces hemolysis effect, due to lower interaction surface with RBC	[51]	Pathology changes: • Both micro- and nano-sized GO cause pulmonary edema and granuloma formation in lung, due to retention time up to 1 month. • Micro-sized GO causes lung occlusion within 1 min.	[58,59,89]
Surfactant	Hemocompatibility: • Surfactant (1% Tween 80) reduces hemolysis effect of GO, due to reduced interaction between GO and blood cells.	[64]	Toxicity: • Surfactant (1% Tween 80) leads to accumulation of GO in liver, due to greater mobility in circulatory system. Pathology changes: • Surfactant (1% Tween 80) leads to no histological alterations of blood cells, spleen, brain and testes by GO.	[64]

Two studies reported that a BSA coating on GO resulted in very little inhibition of cell proliferation at doses up to 50 μg/mL [31,65]. The mitigation behavior might be attributed to the protein adsorbed on GO that weakened the interaction between GO and the cells [66].

In terms of cellular uptake, Mu et al. [31] reported that the internalization of GO/BSA into mouse mesenchymal progenitor (C2C12) cells was complete within 30 min. Although the protein in BSA was not identified, these proteins most likely helped in modulating the uptake. Different sizes of GO/BSA led to different patterns of internalization. The results showed that GO/BSA larger than 500 nm activated phagocytosis, whereas those conjugates smaller than 500 nm entered cells *via* clathrin-mediated endocytosis [31].

3.2. Poly(ethylene glycol) (PEG)

Poly(ethylene glycol) (PEG) is a biocompatible polymer that has been approved for human use by the Food and Drug Administration (FDA). It is non-toxic and can be easily eliminated by the renal or hepatic pathway. PEG is frequently used as a GO coating because it provides good dispersibility of GO in biological solutions [17,48,67,68,93] and it confers stealth properties to the particles it coats. PEG conjugation can prevent the uptake of GO–PEG by macrophages because PEG screens the electrostatic charge of GO [17,77] and also because of the protein-resistant properties of PEG that help to decrease the interaction between GO and biological interfaces [48]. In addition, a covalent coating of PEG on GO also remarkably increased the NIR absorbance of GO at 808 nm, by at least 6-fold due to a chemical reduction reaction that restored the aromatic and conjugated character of GO sheets [67]. Such alterations may provide another advantage to GO for use as a NIR light-induced photothermal agent for anticancer photothermal therapy.

From here onwards, linear PEG and 6-arm branched PEG are termed 1PEG and 6PEG, respectively. GO–1PEG conjugates (~40 nm) were highly biocompatible with A549 cells, in which no toxicity was observed up to a concentration of 100 μg/mL upon 48 h of incubation [17]. In another report, Vila et al. [48] conducted a comparative study on how the number of PEG branches affects the cellular uptake and cytotoxicity effects of GO. The cellular uptake of GO–1PEG (95 nm) was significantly higher than that of GO–6PEG (190 nm) in osteoblasts, fibroblasts and macrophages. The lower cellular uptake of GO–6PEG might be due to the reduced interaction of highly branched PEG with the biological surfaces of the cell [48]. GO–6PEG had lower cell uptake compared with that of GO–1PEG but produced similar effects on cell viability (60% viability at 75 μg/mL), indicating that GO–6PEG could most likely induce different alterations of cell function from those by GO–1PEG [48]. Different types of conjugations (covalent and non-covalent) of PEG with GO showed similar levels of toxicity [67].

3.3. Dextran (DEX)

Dextran (DEX) is a biodegradable natural polymer that can weaken the serum opsonization of GO *in vivo*. DEX has been reported to improve the stability of GO in biological solutions without obvious agglomeration [69]. Three research groups [69–71] coated GO with DEX and observed that GO–DEX was highly compatible with HeLa cells, maintaining more than 80% of the cell viability at concentrations of up to 450 μg/mL [70]. Interestingly, the optical density of GO–DEX in the NIR region (800 nm) was significantly increased by 18.6-fold compared with that of as-prepared GO [69]. This finding again alludes to the promising application of GO–DEX in photothermal therapy. Chen et al. [71] further coated iron oxide (Fe) on GO–DEX to transform it into an MRI contrast agent. The GO–Fe–DEX had negligible toxicity (~100%) although the Fe concentration was as high as 80 μg/mL.

3.4. Poly(amido amine) (PAMAM) dendrimer

Wate et al. [47] constructed a multicomponent nanostructured system — GO–G4–Fe–Cy — that displayed multiple features, such as high payload, magnetic cellular targeting, aqueous dispersibility and fluorescence optical imaging. G4, Fe and Cy represent 4th generation amine-terminated poly(amido amine) dendrimer, Fe_3O_4 and cyanine 5, respectively. The GO–G4–Fe–Cy nanostructured system showed almost no toxic effects on MDA-MB-231 cells at 100 μg/mL but the free PAMAM G4 dendrimer induced 97% cell death. The author claimed that the amine (NH_2) groups on the dendrimer caused the increase in the toxicity of the material [47]. The GO–G4–Fe–Cy nanosystem mainly localized in the cytoplasm of MCF-7 cells after 6 h and then migrated to perinuclear regions after 24 h. The nanosystem resided in cells far longer than did the free Cy, most likely due to the high mobility of small Cy, which allows it to diffuse out of cells. In another study, hydroxyl-terminated PAMAM dendrimer and folic acid were chemically conjugated to GO to produce GO–DEN–OH–FA conjugate [72]. In contrast to the amine-terminated dendrimer, the study found that the hydroxyl-terminated dendrimer had improved biocompatibility with cell viability of more than 70% at 100 μg/mL. Upon irradiation with a laser beam at 780 nm for 15 min, the GO–DEN–OH–FA conjugate induced cell death in HeLa cells. The author claimed that the cells' death was caused by ROS generated from the conjugate upon irradiation, suggesting the presence of phototherapeutic behavior of the GO conjugates.

3.5. Other surface coatings

Pluronic F127 – a triblock amphiphilic copolymer – is an excellent stabilizer for enhancing the dispersibility of GO in aqueous electrolyte solutions, cell culture media and serum [73]. However, GO/F127 exhibited more than 20% toxicity at 0.5 mM polymer, whereas pluronic F127 itself was safe at 4 mM [73]. Improvement of this type of surface coating is needed, and the *in vitro* toxicity profile requires further investigation.

A coating of titanium oxide (TiO_2) on GO helped GO advance into a visible light-driven PDT tool [74]. Under visible light, the GO/TiO_2 (100 μg/mL of GO) semiconductor generated 4-fold more ROS compared with that of GO alone and this led to the apoptosis of HeLa cells. No dark toxicity was observed at the same concentration of GO.

Thus far, PEG and DEX are the two most biocompatible surface coatings for GO. In addition, these coatings provide GO with good dispersibility in biological solutions and enhance the NIR photothermal effect of GO. A PEG coating also helps GO to escape from macrophage recognition.

Table 4 shows the *in vitro* stages and preclinical trials of GO and its derivatives formulated with anticancer drugs (chemotherapeutic drugs and photosensitizers). The principles of chemotherapy and photodynamic therapies have been clearly elaborated [94–97]. It can be seen that the published studies are focusing on chemotherapy drugs and photosensitizers with planar structures that can form a π–π interaction with graphenic domain on GO. Therefore, further studies are required to explore the possibility of loading other hydrophobic drugs with non-planar structures on GO-based nanocarriers.

4. Conclusion — challenges and future perspectives

This paper gives a systematic review on how physicochemical properties of GO and different surface coatings affect the *in vitro* and *in vivo* biocompatibility of GO-based formulations. This article complements previous reviews on the design, synthesis [24,25,27,36], physicochemical properties, biomedical applications [20] and *in vitro* efficacy [2,22,23] of GO.

As described throughout the review, we found that nano-sized GO, especially GO in the range of 100 to 200 nm, can fulfill the majority of the essential requirements of an effective drug carrier. The drawbacks of nano-sized GO for the biocompatibility criteria, such as hemolysis

Table 4
In vitro and preclinical trials of GO-based formulations carrying chemotherapeutic and photodynamic drugs.

GO-based formulation	Drug*/photosensitizer**	Targeting molecule	Size of GO	Cell type and animal model	Ref.
GO	Doxorubicin*	–	~500 nm	–	[19]
	Doxorubicin*	–	–	CNE1 (human nasopharyngeal carcinoma)	[98]
	Doxorubicin*	HA	10–200 nm	HepG2 (human hepatocellular liver carcinoma) RBMEC (rat brain microvascular endothelial cell) H22 hepatic cancer cell-bearing Kunming mice	[81]
	Doxorubicin*, Camptothecin*	FA	~150 nm	MCF-7 (human breast cancer) A549 (human lung adenorcarcinoma cells)	[99]
	Hypocrellin B**	–	–	HeLa (human cervical carcinoma cell) SMMC-7721 (human carcinoma cells) SGC-7901 (human gastric cancer cells) A549 (human lung adenorcarcinoma cells)	[100]
	Chlorin e6**	FA	~500 nm	MGC803 (human stomach cancer)	[101]
GO–6PEG	Doxorubicin*	Rituxan	<10 nm	Raji cells CEM T-cells	[45]
	Doxorubicin*	TFN	100–400 nm	C6 glioma Sprague–Dawley rats	[83]
	Doxorubicin*	IONP	~50–300 nm	4 T1 (murine breast cancer) 4 T1 murine breast tumor-bearing Balb/c mice	[84]
	SN-38*	–	~5–50 nm	HCT-116 (human colon cancer)	[16]
	Paclitaxel*	–	50–200 nm	A549 (human lung adenorcarcinoma cells) MCF-7 (human breast cancer)	[102]
	Chlorin e6**	Herceptin	<50 nm	KB (human nasopharyngeal epidermal carcinoma)	[103]
GO–6PEG–PAH–DA	Doxorubicin*	–	70 nm	MCF-7/WT (wild-type human breast cancer) MCF-7/ADR (drug-resistant human breast cancer)	[104]
GO–1PEG	Doxorubicin*	–	~100 nm	EMT6 (murine mammary tumor line) EMT6 tumor-bearing mice	[86]
GO–Cyt–ALG–1PEG	Doxorubicin*	–	94.7 ± 9.6 nm	HepG2 (human liver carcinoma cell)	[57]
GO–1PEG–Gd	Doxorubicin*	–	100–300 nm	HepG2 (human liver carcinoma cell)	[105]
GO–1PEG	HPPH**	–	<50 nm	4T1 murine breast cancer cell Athymic nude mice	[85]
GO–CS	Doxorubicin*	FA	>5 μm	–	[106]
GO–CS	Camptothecin*	–	~170 nm	HepG2 (human hepatocellular liver carcinoma) HeLa cell	[107]
GO–bPEI	Doxorubicin* Elsinochrome A**	FA	<30 nm	CBRH7919 (rat hepatocellular carcinoma) HL7702 liver cells Primary cultured mouse central neurogliocyte cells	[108]
GO–bPEI–1PEG	Doxorubicin*	–	100–200 nm	PC-3 (human prostate cancer cell HeLa cell (human cervical carcinoma cell)	[49]
GO–PAH	Doxorubicin*	–	~5 μm	MCF-7 (human breast cancer)	[109]
GO/Ag	Doxorubicin*	NGR	–	MCF-7 Balb/c mice S180 tumor model	[87]
GO/Fe	Doxorubicin*	FA	<200 nm	HeLa SK3 (human breast cancer)	[110]
GO/Au	Doxorubicin*	–	~50 nm	–	[111]
GO/DEX–hematin	Doxorubicin*	–	220–240 nm	MCF-7/ADR	[90]

Symbol: GO = graphene oxide, HA = hyaluronic acid, FA = folic acid, 6PEG = branched poly(ethylene glycol), TFN = transferrin, IONP = iron oxide nanoparticle, SN38 = 7-ethyl-10-hydroxy-camptothecin, PAH = poly(allylamine) hydrochloride, DA = 2,3-dimethylmaleic anhydride, 1PEG = linear poly(ethylene glycol), Cyt = cystamine, ALG = alginate, Gd = gadolinium, HPPH = (2-(1-hexyloxyethyl)-2-devinyl pyropheophorbide-alpha), CS = chitosan, bPEI = branched polyethyleneimine, Ag = silver, NGR = Asn-Gly-Arg peptide, Fe = Fe_3O_4 iron oxide, Au = gold nanostar, DEX = dextran. Chemical bonds: — indicates covalent bonding and / indicates noncovalent in the GO-based formulation.
Asterisk: * indicates chemotherapeutic drug and ** indicates photosensitizer.

and clearance issues, can be addressed by choosing appropriate surface coatings, like PEG and DEX.

A recent study reported that GO could selectively target and inhibit the proliferation of cancer stem cells to form tumor-sphere, providing yet another characteristic of a promising therapeutic candidate for targeted drug delivery [112].

However, as-prepared GO rarely appears in uniform sizes, which could greatly affect its *in vitro* and *in vivo* biocompatibility, leading to inconsistency in the results. At this stage, plain GO is known to induce pulmonary toxicity because it has a tendency for high accumulation in the lungs upon injection. Moreover, the bio-persistence of plain GO in the human body could potentially trigger immunology and pathology effects.

Therefore, we note the following challenges that must be met and the progress that is required in the future to propel applications of GO-based carriers into pre-clinical or clinical stages:

- To develop a facile method for reproducible synthesis and meaningful batch-to-batch characterization of GO to accurately control the size and quality.
- To explore the optimum dosage that maintains a balance between the therapeutic effects and nanotoxicity of GO-based formulations.
- To explore the possibility of GO-based formulations carrying other hydrophobic drugs that have limited clinical utility because of their poor solubility.
- To develop a GO-based formulation that can cure lung disease because GO has a strong tendency to accumulate in lungs.
- To explore other surface coatings of GO that have unique properties similar to PEG and DEX.
- To develop a GO-based formulation that can be cleared from the body in a shorter period.
- To evaluate the biocompatibility of GO-based formulations with relevant pre-clinical *in vitro* and *in vivo* models so that the results obtained can easily be translated to clinics.
- To standardize the terminologies used in GO research and validate the toxicological methodologies to give comparable results to elucidate the potential toxicological effects of GO-based formulations.
- To assess the adverse effects of GO based formulations on human and environment as the large scale of production at industrial

level can lead to potential human exposure and environmental issues.

Acknowledgment

We would like to thank HIR-MoHE grants (UM.C/625/1/HIR/MOHE/MED/17 and UM.C/625/1/HIR/MOHE/MED/33) from the Ministry of Higher Education, Malaysia for financial support. SF Kiew is a recipient of MyPhD scholarship from the Ministry of Education, Malaysia.

References

[1] K.S. Novoselov, A.K. Geim, S.V. Morozov, D. Jiang, Y. Zhang, S.V. Dubonos, I.V. Grigorieva, A.A. Firsov, Electric field effect in atomically thin carbon films, Science 306 (2004) 666–669.
[2] G. Hong, S. Diao, A.L. Antaris, H. Dai, Carbon nanomaterials for biological imaging and nanomedicinal therapy, Chem. Rev. 115 (2015) 10816–10906.
[3] T. Kuila, S. Bose, P. Khanra, A.K. Mishra, N.H. Kim, J.H. Lee, Recent advances in graphene-based biosensors, Biosen. Bioelectron. 26 (2011) 4637–4648.
[4] P.J.J. Huang, J. Liu, Molecular beacon lighting up on graphene oxide, Anal. Chem. 84 (2012) 4192–4198.
[5] S. Bykkam, K. V.R., C.H. S.C., T. Thunugunta, Synthesis and characterization of graphene oxide and its antimicrobial activity against *Klebsiella* and *Staphylococcus*, Int. J. Adv. Biotechnol. Res. 4 (2013) 142–146.
[6] K. Yang, S. Zhang, G. Zhang, X. Sun, S.T. Lee, Z. Liu, Graphene in mice: ultrahigh in vivo tumor uptake and efficient photothermal therapy, Nano Lett. 10 (2010) 3318–3323.
[7] C. Shan, H. Yang, D. Han, Q. Zhang, A. Ivaska, L. Niu, Water-soluble graphene covalently functionalized by biocompatible poly-L-lysine, Langmuir 25 (2009) 12030–12033.
[8] Z. Wang, P. Huang, A. Bhirde, A. Jin, Y. Ma, G. Niu, N. Neamati, X. Chen, A nanoscale graphene oxide–peptide biosensor for real-time specific biomarker detection on the cell surface, Chem. Commun. 48 (2012) 9768–9770.
[9] M. Zhang, B.bC. Yin, X.F. Wang, B.C. Ye, Interaction of peptides with graphene oxide and its application for real-time monitoring of protease activity, Chem. Commun. 47 (2011) 2399–2401.
[10] M. Mehrali, E. Moghaddam, S.F. Seyed Shirazi, S. Baradaran, M. Mehrali, S. Tahan Latibari, H.S. Metselaar, N.A. Kadri, K. Zandi, N.A. Abu Osman, Synthesis, mechanical properties and in vitro biocompatibility with osteoblasts of calcium silicate–reduced graphene oxide composites, ACS Appl. Mater. Interfaces 6 (2014) 3947–3962.
[11] S. Sreejith, X. Ma, Y. Zhao, Graphene oxide wrapping on squaraine-loaded mesoporous silica nanoparticles for bioimaging, J. Am. Chem. Soc. 134 (2012) 17346–17349.
[12] S.K. Tripathi, R. Goyal, K.C. Gupta, P. Kumar, Functionalized graphene oxide mediated nucleic acid delivery, Carbon 51 (2013) 224–235.
[13] C. Bussy, H. Ali-Boucetta, K. Kostarelos, Safety considerations for graphene: lessons learnt from carbon nanotubes, Acc. Chem. Res. 46 (2013) 692–701.
[14] S. Kang, M. Pinault, L.D. Pfefferle, M. Elimelech, Single-walled carbon nanotubes exhibit strong antimicrobial activity, Langmuir 23 (2007) 8670–8673.
[15] T. Kuila, S. Bose, A.K. Mishra, P. Khanra, N.H. Kim, J.H. Lee, Chemical functionalization of graphene and its applications, Prog. Mater. Sci. 57 (2012) 1061–1105.
[16] Z. Liu, J.T. Robinson, X. Sun, H. Dai, PEGylated nanographene oxide for delivery of water-insoluble cancer drugs, J. Am. Chem. Soc. 130 (2008) 10876–10877.
[17] X. Zhang, R. Yang, C. Wang, C.L. Heng, Cell biocompatibility of functionalized graphene oxide, Acta Phys. -Chim. Sin. 28 (2012) 1520–1524.
[18] Y. Pan, N.G. Sahoo, L. Li, The application of graphene oxide in drug delivery, Expert Opin. Drug Deliv. 9 (2012) 1365–1376.
[19] X. Yang, X. Zhang, Z. Liu, Y. Ma, Y. Huang, Y. Chen, High-efficiency loading and controlled release of doxorubicin hydrochloride on graphene oxide, J. Phys. Chem. C 112 (2008) 17554–17558.
[20] S. Goenka, V. Sant, S. Sant, Graphene-based nanomaterials for drug delivery and tissue engineering, J. Control. Release 173 (2014) 75–88.
[21] J.R. Potts, D.R. Dreyer, C.W. Bielawski, R.S. Ruoff, Graphene-based polymer nanocomposites, Polymer 52 (2011) 5–25.
[22] Y. Ma, H. Shen, X. Tu, Z. Zhang, Assessing in vivo toxicity of graphene materials: current methods and future outlook, Nanomedicine 9 (2014) 1565–1580.
[23] V.C. Sanchez, A. Jacjak, R.H. Hurt, A.B. Kane, Biological interactions of graphene-family nanomaterials: an interdisciplinary review, Chem. Res. Toxicol. 25 (2012) 15–34.
[24] P.T. Yin, S. Shah, M. Chhowalla, K.-B. Lee, Design, synthesis, and characterization of graphene–nanoparticle hybrid materials for bioapplications, Chem. Rev. 115 (2015) 2483–2531.
[25] S. Shi, F. Chen, E.B. Ehlerding, W. Cai, Surface engineering of graphene-based nanomaterials for biomedical applications, Bioconjug. Chem. 25 (2014) 1609–1619.
[26] C. Fisher, A.E. Rider, Z.J. Han, S. Kumar, I. Levchenko, K. Ostrikov, Applications and nanotoxicity of carbon nanotubes and graphene in biomedicine, J. Nanomater. 2012 (2012) 1–19.
[27] Y. Wang, Z. Li, J. Wang, J. Li, Y. Lin, Graphene and graphene oxide: biofunctionalization and applications in biotechnology, Trends Biotechnol. 29 (2011) 205–212.
[28] H. Shen, L. Zhang, M. Liu, Z. Zhang, Biomedical applications of graphene, Theranostics 2 (2012) 283–294.
[29] D.R. Dreyer, S. Park, C.W. Bielawski, R.S. Ruoff, The chemistry of graphene oxide, Chem. Soc. Rev. 39 (2010) 228–240.
[30] A. Lerf, H. He, M. Forster, J. Klinowski, Structure of graphite oxide revisited, J. Phys. Chem. B 102 (1998) 4477–4482.
[31] Q. Mu, G. Su, L. Li, B.O. Gilbertson, L.H. Yu, Q. Zhang, Y.P. Sun, B. Yan, Size-dependent cell uptake of protein-coated graphene oxide nanosheets, ACS Appl. Mater. Interfaces 4 (2012) 2259–2266.
[32] J.I. Paredes, S. Villar-Rodil, A. Martínez-Alonso, J.M.D. Tascón, Graphene oxide dispersions in organic solvents, Langmuir 24 (2008) 10560–10564.
[33] H. Yue, W. Wei, Z. Yue, B. Wang, N. Luo, Y. Gao, D. Ma, G. Ma, Z. Su, The role of the lateral dimension of graphene oxide in the regulation of cellular responses, Biomaterials 33 (2012) 4013–4021.
[34] H. Zhang, C. Peng, J. Yang, M. Lv, R. Liu, D. He, C. Fan, Q. Huang, Uniform ultrasmall graphene oxide nanosheets with low cytotoxicity and high cellular uptake, ACS Appl. Mater. Interfaces 5 (2013) 1761–1767.
[35] R. Yang, Z. Tang, J. Yan, H. Kang, Y. Kim, Z. Zhu, W. Tan, Noncovalent assembly of carbon nanotubes and single-stranded DNA: an effective sensing platform for probing biomolecular interactions, Anal. Chem. 80 (2008) 7408–7413.
[36] M. Hakimi, P. Alimard, Graphene: synthesis and applications in biotechnology — a review, World Appl. Program. 2 (2012) 377–388.
[37] H. Hu, J. Yu, Y. Li, J. Zhao, H. Dong, Engineering of a novel pluronic f127/graphene nanohybrid for pH responsive drug delivery, J. Biomed. Mater. Res. A 100 (2011) 141–148.
[38] R. Zhang, M. Hummelgard, G. Lv, H. Olin, Real time monitoring of the drug release of rhodamine B on graphene oxide, Carbon 49 (2011) 1126–1132.
[39] S. Kim, Y. Shi, J.Y. Kim, K. Park, J.X. Cheng, Overcoming the barriers in micellar drug delivery: loading efficiency, in vivo stability, and micelle–cell interaction, Expert Opin. Drug Deliv. 7 (2010) 49–62.
[40] W. Sun, N. Zhang, A. Li, W. Zou, W. Xu, Preparation and evaluation of N3-O-toluyl-fluorouracil-loaded liposomes, Int. J. Pharm. 353 (2008) 243–250.
[41] G. Xie, J. Cheng, Y. Li, P. Xi, F. Chen, H. Liu, F. Hou, Y. Shi, L. Huang, Z. Xu, D. Bai, Z. Zeng, Fluorescent graphene oxide composites synthesis and its biocompatibility study, J. Mater. Chem. 22 (2012) 9308.
[42] D. Li, M.B. Müller, S. Gilje, R.B. Kaner, G.G. Wallace, Processable aqueous dispersions of graphene nanosheets, Nat. Nanotechnol. 3 (2008) 101–105.
[43] O.N. Ruiz, K.A.S. Fernando, B. Wang, N.A. Brown, P.G. Luo, N.D. McNamara, M. Vangsness, Y.P. Sun, C.E. Bunker, Graphene oxide: a nonspecific enhancer of cellular growth, ACS Nano 5 (2011) 8100–8107.
[44] J.T. Chen, Y.J. Fu, Q.F. An, S.C. Lo, S.H. Huang, W.S. Hung, C.C. Hu, K.R. Lee, J.Y. Lai, Tuning nanostructure of graphene oxide/polyelectrolyte LbL assemblies by controlling pH of GO suspension to fabricate transparent and super gas barrier films, Nanoscale 5 (2013) 9081–9088.
[45] X. Sun, Z. Liu, K. Welsher, J.T. Robinson, A. Goodwin, S. Zaric, H. Dai, Nano-graphene oxide for cellular imaging and drug delivery, Nano Res. 1 (2008) 203–212.
[46] H.Y. Mao, S. Laurent, W. Chen, O. Akhavan, M. Imani, A.A. Ashkarran, M. Mahmoudi, Graphene: promises, facts, opportunities, and challenges in nanomedicine, Chem. Rev. 113 (2013) 3407–3424.
[47] P.S. Wate, S.S. Banerjee, A. Jalota-Badhwar, R.R. Mascarenhas, K.R. Zope, J. Khandare, R.D. Misra, Cellular imaging using biocompatible dendrimer-functionalized graphene oxide-based fluorescent probe anchored with magnetic nanoparticles, Nanotechnology 23 (2012) 415101–415108.
[48] M. Vila, M.T. Portoles, P.A.A.P. Marques, M.J. Feito, M.C. Matesanz, C. Ramirez-Santillan, G. Goncalves, S.M.A. Cruz, A. Nieto, M. Vallet-Regi, Cell uptake survey of pegylated nanographene oxide, Nanotechnology 23 (2012) 9.
[49] H. Kim, D. Lee, J. Kim, T.-i. Kim, W.J. Kim, Photothermally triggered cytosolic drug delivery via endosome disruption using a functionalized reduced graphene oxide, ACS Nano 7 (2013) 6735–6746.
[50] I. Chowdhury, M.C. Duch, N.D. Mansukhani, M.C. Hersam, D. Bouchard, Deposition and release of graphene oxide nanomaterials using a quartz crystal microbalance, Environ. Sci. Technol. 48 (2013) 961–969.
[51] K.H. Liao, Y.S. Lin, W.M. Christopher, C.L. Haynes, Cytotoxicity of graphene oxide and graphene in human erythrocytes and skin fibroblasts, ACS Appl. Mater. Interfaces 3 (2011) 2607–2615.
[52] E.M. Martín del Valle, M.A. Galán, R.G. Carbonell, Drug delivery technologies: the way forward in the new decade, Ind. Eng. Chem. Res. 48 (2009) 2475–2486.
[53] D. He, X. He, K. Wang, Z. Zou, X. Yang, X. Li, Remote-controlled drug release from graphene oxide-capped mesoporous silica to cancer cells by photoinduced pH-jump activation, Langmuir 30 (2014) 7182–7189.
[54] C.L. Weaver, J.M. LaRosa, X. Luo, X.T. Cui, Electrically controlled drug delivery from graphene oxide nanocomposite films, ACS Nano 8 (2014) 1834–1843.
[55] R. Kurapati, A.M. Raichur, Near-infrared light-responsive graphene oxide composite multilayer capsules: a novel route for remote controlled drug delivery, Chem. Commun. 49 (2013) 734–736.
[56] M. Kakran, N.G. Sahoo, H. Bao, Y. Pan, L. Li, Functionalized graphene oxide as nanocarrier for loading and delivery of ellagic acid, Curr. Med. Chem. 18 (2011) 4503–4512.
[57] X. Zhao, L. Liu, X. Li, J. Zeng, X. Jia, P. Liu, Biocompatible graphene oxide nanoparticle-based drug delivery platform for tumor microenvironment-responsive triggered release of doxorubicin, Langmuir 30 (2014) 10419–10429.
[58] K. Wang, J. Ruan, H. Song, J. Zhang, Y. Wo, S. Guo, D. Cui, Biocompatibility of graphene oxide, Nanoscale Res. Lett. 23 (2011) 1–8.
[59] X. Zhang, J. Yin, C. Peng, W. Hu, Z. Zhu, W. Li, C. Fan, Q. Huang, Distribution and biocompatibility studies of graphene oxide in mice after intravenous administration, Carbon 49 (2011) 986–995.
[60] A.V. Titov, P. Král, R. Pearson, Sandwiched graphene — membrane superstructures, ACS Nano 4 (2009) 229–234.

[61] P. Wick, A.E. Louw-Gaume, M. Kucki, H.F. Krug, K. Kostarelos, B. Fadeel, K.A. Dawson, A. Salvati, E. Vazquez, L. Ballerini, M. Tretiach, F. Benfenati, E. Flahaut, L. Gauthier, M. Prato, A. Bianco, Classification framework for graphene-based materials, Angew. Chem. 53 (2014) 7714–7718.
[62] L. Yan, Y. Wang, X. Xu, C. Zeng, J. Hou, M. Lin, J. Xu, F. Sun, X. Huang, L. Dai, F. Lu, Y. Liu, Can graphene oxide cause damage to eyesight? Chem. Res. Toxicol. 25 (2012) 1265–1270.
[63] Y. Chang, S.T. Yang, J.H. Liu, E. Dong, Y. Wang, A. Cao, Y. Liu, H. Wang, In vitro toxicity evaluation of graphene oxide on A549 cells, Toxicol. Lett. 200 (2011) 201–210.
[64] G. Qu, X. Wang, Q. Liu, R. Liu, N. Yin, J. Ma, L. Chen, J. He, S. Liu, G. Jiang, The ex vivo and in vivo biological performances of graphene oxide and the impact of surfactant on graphene oxide's biocompatibility, J. Environ. Sci. 25 (2013) 873–881.
[65] C. Cheng, S. Nie, S. Li, H. Peng, H. Yang, L. Ma, S. Sun, C. Zhao, Biopolymer functionalized reduced graphene oxide with enhanced biocompatibility via mussel inspired coatings/anchors, J. Mater. Chem. B 1 (2013) 265–275.
[66] W. Hu, C. Peng, M. Lv, X. Li, Y. Zhang, N. Chen, C. Fan, Q. Huang, Protein corona-mediated mitigation of cytotoxicity of graphene oxide, ACS Nano 5 (2011) 3693–3700.
[67] J.T. Robinson, S.M. Tabakman, Y. Liang, H. Wang, H.S. Casalongue, D. Vinh, H. Dai, Ultrasmall reduced graphene oxide with high near-infrared absorbance for photothermal therapy, J. Am. Chem. Soc. 133 (2011) 6825–6831.
[68] H. Hong, K. Yang, Y. Zhang, J.W. Engle, L. Feng, Y. Yang, T.R. Nayak, S. Goel, J. Bean, C.P. Theuer, T.E. Barnhart, Z. Liu, W. Cai, In vivo targeting and imaging of tumor vasculature with radiolabeled antibody-conjugated nanographene, ACS Nano 6 (2012) 2361–2370.
[69] S. Zhang, K. Yang, L. Feng, Z. Liu, In vitro and in vivo behaviors of dextran functionalized graphene, Carbon 49 (2011) 4040–4049.
[70] Y.K. Kim, M.H. Kim, D.H. Min, Biocompatible reduced graphene oxide prepared by using dextran as a multifunctional reducing agent, Chem. Commun. 47 (2011) 3195–3197.
[71] W. Chen, P. Yi, Y. Zhang, L. Zhang, Z. Deng, Z. Zhang, Composites of aminodextran-coated Fe_3O_4 nanoparticles and graphene oxide for cellular magnetic resonance imaging, ACS Appl. Mater. Interfaces 3 (2011) 4085–4091.
[72] A. Siriviriyanun, T. Imae, G. Calderó, C. Solans, Phototherapeutic functionality of biocompatible graphene oxide/dendrimer hybrids, Colloids Surf. B 121 (2014) 469–473.
[73] B.J. Hong, O.C. Compton, Z. An, I. Eryazici, S.T. Nguyen, Successful stabilization of graphene oxide in electrolyte solutions: enhancement of biofunctionalization and cellular uptake, ACS Nano 6 (2011) 63–73.
[74] Z. Hu, Y. Huang, S. Sun, W. Guan, Y. Yao, P. Tang, C. Li, Visible light driven photodynamic anticancer activity of graphene oxide/TiO_2 hybrid, Carbon 50 (2012) 994–1004.
[75] S. Liu, L. Wei, L. Hao, N. Fang, M.W. Chang, R. Xu, Y. Yang, Y. Chen, Sharper and faster "nano darts" kill more bacteria: a study of antibacterial activity of individually dispersed pristine single-walled carbon nanotube, ACS Nano 3 (2009) 3891–3902.
[76] J. Ma, R. Liu, X. Wang, Q. Liu, Y. Chen, R.P. Valle, Y.Y. Zuo, T. Xia, S. Liu, Crucial role of lateral size for graphene oxide in activating macrophages and stimulating pro-inflammatory responses in cells and animals, ACS Nano 9 (2015) 10498–10515.
[77] S. Stolnik, L. Illum, S.S. Davis, Long circulating microparticulate drug carriers, Adv. Drug Deliv. Rev. 16 (1995) 195–214.
[78] Y. Li, Q. Wu, Y. Zhao, Y. Bai, P. Chen, T. Xia, D. Wang, Response of microRNAs to in vitro treatment with graphene oxide, ACS Nano 8 (2014) 2100–2110.
[79] K. Yin Win, S.-S. Feng, Effects of particle size and surface coating on cellular uptake of polymeric nanoparticles for oral delivery of anticancer drugs, Biomaterials 26 (2005) 2713–2722.
[80] B. Cornelissen, S. Able, V. Kersemans, P.A. Waghorn, S. Myhra, K. Jurkshat, A. Crossley, K.A. Vallis, Nanographene oxide-based radioimmunoconstructs for in vivo targeting and SPECT imaging of HER2-positive tumors, Biomaterials 34 (2013) 1146–1154.
[81] E. Song, W. Han, C. Li, D. Cheng, L. Li, L. Liu, G. Zhu, Y. Song, W. Tan, Hyaluronic acid-decorated graphene oxide nanohybrids as nanocarriers for targeted and pH-responsive anticancer drug delivery, ACS Appl. Mater. Interfaces 6 (2014) 11882–11890.
[82] K. Yang, H. Gong, X. Shi, J. Wan, Y. Zhang, Z. Liu, In vivo biodistribution and toxicology of functionalized nano-graphene oxide in mice after oral and intraperitoneal administration, Biomaterials 34 (2013) 2787–2795.
[83] G. Liu, H. Shen, J. Mao, L. Zhang, Z. Jiang, T. Sun, Q. Lan, Z. Zhang, Transferrin modified graphene oxide for glioma-targeted drug delivery: in vitro and in vivo evaluations, ACS Appl. Mater. Interfaces 5 (2013) 6909–6914.
[84] X. Ma, H. Tao, K. Yang, L. Feng, L. Cheng, X. Shi, Y. Li, L. Guo, Z. Liu, A functionalized graphene oxide-iron oxide nanocomposite for magnetically targeted drug delivery, photothermal therapy, and magnetic resonance imaging, Nano Res. 5 (2012) 199–212.
[85] P. Rong, K. Yang, A. Srivastan, D.O. Kiesewetter, X. Yue, F. Wang, L. Nie, A. Bhirde, Z. Wang, Z. Liu, G. Niu, W. Wang, X. Chen, Photosensitizer loaded nano-graphene for multimodality imaging guided tumor photodynamic therapy, Theranostics 4 (2014) 229–239.
[86] W. Zhang, Z. Guo, D. Huang, Z. Liu, X. Guo, H. Zhong, Synergistic effect of chemo-photothermal therapy using PEGylated graphene oxide, Biomaterials 32 (2011) 8555–8561.
[87] J. Shi, L. Wang, J. Zhang, R. Ma, J. Gao, Y. Liu, C. Zhang, Z. Zhang, A tumor-targeting near-infrared laser-triggered drug delivery system based on GO@Ag nanoparticles for chemo-photothermal therapy and X-ray imaging, Biomaterials 35 (2014) 5847–5861.
[88] J. Jeong, H.-J. Cho, M. Choi, W.S. Lee, B.H. Chung, J.-S. Lee, In vivo toxicity assessment of angiogenesis and the live distribution of nano-graphene oxide and its PEGylated derivatives using the developing zebrafish embryo, Carbon 93 (2015) 431–440.
[89] S.A. Sydlik, S. Jhunjhunwala, M.J. Webber, D.G. Anderson, R. Langer, In vivo compatibility of graphene oxide with differing oxidation states, ACS Nano 9 (2015) 3866–3874.
[90] R. Jin, X. Ji, Y. Yang, H. Wang, A. Cao, Self-assembled graphene–dextran nanohybrid for killing drug-resistant cancer cells, ACS Appl. Mater. Interfaces 5 (2013) 7181–7189.
[91] L. Feng, Z. Liu, Graphene in biomedicine: opportunities and challenges, Nanomedicine 6 (2011) 317–324.
[92] A. Lesniak, F. Fenaroli, M.P. Monopoli, C. Åberg, K.A. Dawson, A. Salvati, Effects of the presence or absence of a protein corona on silica nanoparticle uptake and impact on cells, ACS Nano 6 (2012) 5845–5857.
[93] H. Shen, M. Liu, H. He, L. Zhang, J. Huang, Y. Chong, J. Dai, Z. Zhang, PEGylated graphene oxide-mediated protein delivery for cell function regulation, ACS Appl. Mater. Interfaces 4 (2012) 6317–6323.
[94] V. Malhotra, M.C. Perry, Classical chemotherapy: mechanisms, toxicities and the therapeutic window, Cancer Biol. Ther. 2 (2003) S2–S4.
[95] J.A. McKnight, Principles of chemotherapy, Clin. Tech. Small Anim. Pract. 18 (2003) 67–72.
[96] S.B. Brown, E.A. Brown, I. Walker, The present and future role of photodynamic therapy in cancer treatment, Lancet Oncol. 5 (2004) 497–508.
[97] J. Moan, K. Berg, The photodegradation of porphyrins in cells can be used to estimate the lifetime of singlet oxygen, Photochem. Photobiol. 53 (1991) 549–553.
[98] D. Ma, J. Lin, Y. Chen, W. Xue, L.-M. Zhang, In situ gelation and sustained release of an antitumor drug by graphene oxide nanosheets, Carbon 50 (2012) 3001–3007.
[99] L. Zhang, J. Xia, Q. Zhao, L. Liu, Z. Zhang, Functional graphene oxide as a nanocarrier for controlled loading and targeted delivery of mixed anticancer drugs, Small 6 (2010) 537–544.
[100] L. Zhou, H. Jiang, S. Wei, X. Ge, J. Zhou, J. Shen, High-efficiency loading of hypocrellin B on graphene oxide for photodynamic therapy, Carbon 50 (2012) 5594–5604.
[101] P. Huang, C. Xu, J. Lin, C. Wang, X. Wang, C. Zhang, X. Zhou, S. Guo, D. Cui, Folic acid-conjugated graphene oxide loaded with photosensitizers for targeting photodynamic therapy, Theranostics 1 (2011) 240–250.
[102] Z. Xu, S. Wang, Y. Li, M. Wang, P. Shi, X. Huang, Covalent functionalization of graphene oxide with biocompatible poly(ethylene glycol) for delivery of paclitaxel, ACS Appl. Mater. Interfaces 6 (2014) 17268–17276.
[103] B. Tian, C. Wang, S. Zhang, L. Feng, Z. Liu, Photothermally enhanced photodynamic therapy delivered by nano-graphene oxide, ACS Nano 5 (2011) 7000–7009.
[104] L. Feng, K. Li, X. Shi, M. Gao, J. Liu, Z. Liu, Smart pH-responsive nanocarriers based on nano-graphene oxide for combined chemo- and photothermal therapy overcoming drug resistance, Adv. Healthcare Mater. 3 (2014) 1261–1271.
[105] M. Zhang, Y. Cao, Y. Chong, Y. Ma, H. Zhang, Z. Deng, C. Hu, Z. Zhang, Graphene oxide based theranostic platform for T1-weighted magnetic resonance imaging and drug delivery, ACS Appl. Mater. Interfaces 5 (2013) 13325–13332.
[106] D. Depan, J. Shah, R.D.K. Misra, Controlled release of drug from folate-decorated and graphene mediated drug delivery system: synthesis, loading efficiency, and drug release response, Mater. Sci. Eng. C 31 (2011) 1305–1312.
[107] H. Bao, Y. Pan, Y. Ping, N.G. Sahoo, T. Wu, L. Li, J. Li, L.H. Gan, Chitosan-functionalized graphene oxide as a nanocarrier for drug and gene delivery, Small 7 (2011) 1569–1578.
[108] G. Wei, M. Yan, R. Dong, D. Wang, X. Zhou, J. Chen, J. Hao, Covalent modification of reduced graphene oxide by means of diazonium chemistry and use as a drug-delivery system, Chem. Eur. J. 18 (2012) 14708–14716.
[109] R. Kurapati, A.M. Raichur, Graphene oxide based multilayer capsules with unique permeability properties: facile encapsulation of multiple drugs, Chem. Commun. 48 (2012) 6013–6015.
[110] X. Yang, W. Yinsong, X. Huang, Y. Ma, Y. Huang, R. Yang, H. Duan, Y. Chen, Multifunctionalized graphene oxide based anticancer drug-carrier with dual-targeting function and pH-sensitivity, J. Mater. Chem. 21 (2011) 3448–3454.
[111] Y. Wang, L. Polavarapu, L.M. Liz-Marzán, Reduced graphene oxide-supported gold nanostars for improved SERS sensing and drug delivery, ACS Appl. Mater. Interfaces 6 (2014) 21798–21805.
[112] M. Fiorillo, A.F. Verre, M. Iliut, M. Peiris-Pages, B. Ozsvari, R. Gandara, A.R. Cappello, F. Sotgia, A. Vijayaraghavan, M.P. Lisanti, Graphene oxide selectively targets cancer stem cells, across multiple tumor types: implications for non-toxic cancer treatment, via "differentiation-based nano-therapy", Oncotarget 6 (2015) 3553–3562.